AN APPLICATION OF 3-D KINEMATICAL CONSERVATION LAWS: PROPAGATION OF A THREE DIMENSIONAL WAVEFRONT

K. R. ARUN, M. LUKÁČOVÁ-MEDVIĎOVÁ, AND S. V. RAGHURAMA RAO

Abstract. We use the newly formulated 3-D kinematical conservation laws (KCL) to study the propagation of a three dimensional nonlinear wavefront in a polytropic gas in a uniform state and at rest in order to test the numerical efficacy of the 3-D KCL theory. We take initial shape of the front to be cylindrically symmetric with a suitable amplitude distribution and let it evolve according to the 3-D weakly nonlinear ray theory (WNLRT), which is obtained by adding to 3-D KCL a transport equation (in conservation form) for small amplitude. The 3-D WNLRT is a weakly hyperbolic 7×7 system that is highly nonlinear. Due to a possibility of appearance of δ waves and shocks it is a challenging task to develop an appropriate numerical method. Here we use the Lax-Friedrichs scheme and Nessyahu-Tadmor central scheme and have obtained some very interesting shapes of the wavefronts for some cases - in one case a kink line and another case a point singularity appear in the physical space though the results remain single valued in the ray coordinates. Thus we find the 3-D KCL to be suitable to solve many complex problems for which there seems to be no other method at present which can give these physically realistic features.

1. Introduction

Propagation of a curved nonlinear wavefront or a shock front exhibits a very complex phenomenon of possessing curves of discontinuity across which the normal to the front and the amplitude distribution on it are discontinuous. Some of these curves of discontinuity are called kinks. A kink is a shock in a corresponding ray coordinate system in which a physically realistic system of conservation laws has been formulated. The conservation form of equations of a curve evolving in two space dimensions is first derived by Morton, Prasad and Ravindran [22] and these new set of conservation laws are termed as kinematical conservation laws (KCL). The KCL being a pure geometrical result, does not take into consideration any dynamics of the propagating front. This makes the KCL an incomplete system. The closure equation for KCL can be derived by considering the dynamical conditions of the propagating front. Prasad and collaborators have used the KCL along with some closure equations derived on physical considerations to solve several interesting problems such as sonic boom signature, tracing nonlinear wavefronts or shock fronts, see [3, 5, 21, 26] for more details.

The KCL for a surface evolving in three space dimensions (called 3-D KCL), a system of 6 conservation laws, were first obtained by Giles, Prasad and Ravindran [12]. Later on the analysis of 3-D KCL is completed by Arun and Prasad [2] and they also formulate 3-D weakly nonlinear ray theory (WNLRT) by adding to 3-D KCL a closure equation in conservation form representing the energy transport

Date: May 22, 2008.

2000 *Mathematics Subject Classification.* Primary 35L65, 35L67; Secondary 35L80.

Key words and phrases. kinematical conservation laws, ray theory, nonlinear waves, kinks, weakly hyperbolic system, finite difference scheme.

equation of a weakly nonlinear ray theory (WNLRT) in three space dimensions. It has been shown in [2] that the 3-D WNLRT is a weakly hyperbolic system; in the sense that the system of equations has an eigenvalue 0 of multiplicity 5, but the associated eigenspace is only 4-dimensional.

Theory of weakly hyperbolic system is an active area of research, [10, 17, 19, 20, 27, 29] since the last 15 years but it is very much incomplete. Appearance of δ waves and δ shocks in the solution of such systems make the numerical approximation of weakly hyperbolic system very complex, see [11]. The main aim of this paper is not to do an intensive computation on the problem of three dimensional nonlinear wavefront but to test the numerical efficacy of the 3-D KCL theory using 3-D WNLRT equations.

In order to demonstrate the applicability of the 3-D KCL theory using 3-D WLNRT for modelling of time evolution of nonlinear wavefronts we present some illustrating numerical experiments. For numerical approximation we have used both the fist order staggered Lax-Friedrichs scheme and the second order Nessyahu-Tadmor scheme. Results obtained by these methods are found to agree very well. The numerical methods have been applied to study the time evolution of a nonlinear wavefront which has initially both concave and convex parts. We have obtained some very interesting shapes of the wavefronts for two cases - in one case a kink line and another case a point singularity appear in the physical space though the results remain single valued in the ray coordinates, as expected for a system of conservation laws. Thus we find the 3-D KCL to be suitable to solve many complex problems for which there seems to be no other method at present which can give such physically realistic features on a moving surface. We plan to investigate 3D KCL theoretically as well as experimentally in future and report the results in a subsequence paper.

2. 3-D Kinematical Conservation Laws

Consider a one parameter family of surfaces in (x_1, x_2, x_3)-space such that it represents the successive positions of a moving surface Ω_t as time varies. Associated with the family, we have a ray velocity $\boldsymbol{\chi}$ at any point (x_1, x_2, x_3) on the surface Ω_t. We consider only the isotropic evolution of Ω_t so that we take $\boldsymbol{\chi}$ to be in the direction of the unit normal $\mathbf{n}$ to Ω_t, i.e, $\boldsymbol{\chi}$=$m\mathbf{n}$, where m is the normal velocity of propagation of Ω_t. We introduce a ray coordinate system (ξ_1, ξ_2, t) such that for t = const. ξ_1 and ξ_2 are surface coordinates on Ω_t. Further, ξ_1 = const., ξ_2 = const. represent the rays, that is a two parameter family of curves orthogonal to Ω_t. Let $\mathbf{u}$ and $\mathbf{v}$ be unit tangent vectors to the curves ξ_2 = const. and ξ_1 = const. on Ω_t, respectively and let $\mathbf{n}$ be a unit normal to Ω_t. Then we have

$$\mathbf{n} = \frac{\mathbf{u} \times \mathbf{v}}{|\mathbf{u} \times \mathbf{v}|}. \tag{2.1}$$

Let an element of distance along a curve (ξ_2 = const., t = const.) be $g_1 \mathrm{d}\xi_1$. Analogously, denote by $g_2 \mathrm{d}\xi_2$ the element of distance along a curve (ξ_1 = const., t = const.) and by $m\mathrm{d}t$ the element of distance along a ray (ξ_1 = const., ξ_2 = const.). Based on geometrical considerations we can derive the KCL [2], [12]

$$(g_1\mathbf{u})_t - (m\mathbf{n})_{\xi_1} = 0, \tag{2.2}$$

$$(g_2\mathbf{v})_t - (m\mathbf{n})_{\xi_2} = 0 \tag{2.3}$$

subject to the condition

$$(g_1\mathbf{u})_{\xi_1} - (g_2\mathbf{v})_{\xi_2} = 0. \tag{2.4}$$

Note that if the relation (2.4) is satisfied at time $t = 0$, then the equations (2.2)-(2.3) imply that it is satisfied for every time t. The kinematical conservation laws

(2.2)-(2.3) are physically realistic in the sense that they represent the conservation of distance in x_1, x_2 and x_3 directions. The KCL (2.2)-(2.3), being six equations in seven unknowns $u_1, u_2, v_1, v_2, m, g_1, g_2$, is an underdetermined system. We use the closure equation by considering the energy propagation along rays of a weakly nonlinear ray theory (WNLRT), see [2], [24] for a comprehensive treatment of this idea. The energy transport equation of WNLRT for a polytropic gas initially at rest and in uniform state can be written in the conservation form

$$\Big((m-1)^2 e^{2(m-1)} g_1 g_2 \sin\chi\Big)_t = 0, \tag{2.5}$$

where χ is the angle between the vectors $\mathbf{u}$ and $\mathbf{v}$. The system of equations (2.2)-(2.3) and (2.5) is the complete set of conservation laws of WNLRT describing the evolution of a nonlinear wavefront Ω_t, cf. [2].

A quasilinear form of the system of equations (2.2)-(2.3) and (2.5) reads

$$AU_t + B^{(1)}U_{\xi_1} + B^{(2)}U_{\xi_2} = 0, \tag{2.6}$$

where $U = (u_1, u_2, v_1, v_2, m, g_1, g_2)$. The expressions for the matrices $A, B^{(1)}$ and $B^{(2)}$ are given in [2]. We would like to point out that the eigenvalues of the system (2.6) are $\lambda_1, \lambda_2(=-\lambda_1), \lambda_3 = \cdots = \lambda_7 = 0$ with only 4 independent eigenvectors for the eigenvalue 0, see [2] for more details. Note that λ_1 is real for $m > 1$ and purely imaginary for $m < 1$. The goal of this paper is to consider the case of $m > 1$.

3. Method of Solution

It has been shown in [2] that the KCL (2.2)-(2.3), obtained purely on geometrical considerations, are equivalent to the ray equations derived from the eikonal equation

$$\varphi_t + m|\nabla\varphi| = 0. \tag{3.1}$$

The first three of the ray equations corresponding to the eikonal equation (3.1) are

$$\frac{\mathrm{d}\mathbf{x}}{\mathrm{d}t} = m\mathbf{n}. \tag{3.2}$$

To study the wave propagation, we consider a wavefront moving into a gas at rest. Let

$$\Omega_0 \colon \mathbf{x}(\xi_1, \xi_2, 0) = \mathbf{x}_0(\xi_1, \xi_2) \tag{3.3}$$

be the initial wavefront with an amplitute distribution

$$m(\xi_1, \xi_2, 0) = m_0(\xi_1, \xi_2). \tag{3.4}$$

Following [2] we can choose the ray coordinates $(\xi_1, \xi_2) = (x_1, x_2)$ at time $t = 0$. The initial values for $g_1, g_2, \mathbf{u}$ and $\mathbf{v}$ are given as

$$g_1(\xi_1, \xi_2, 0) = g_{10} = \left|\frac{\partial \mathbf{x}_0}{\partial \xi_1}\right|, \quad \mathbf{u}(\xi_1, \xi_2, 0) = \mathbf{u}_0 = \frac{1}{g_{10}}\frac{\partial \mathbf{x}_0}{\partial \xi_1}. \tag{3.5}$$

$$g_2(\xi_1, \xi_2, 0) = g_{20} = \left|\frac{\partial \mathbf{x}_0}{\partial \xi_2}\right|, \quad \mathbf{v}(\xi_1, \xi_2, 0) = \mathbf{v}_0 = \frac{1}{g_{20}}\frac{\partial \mathbf{x}_0}{\partial \xi_2}. \tag{3.6}$$

The system of conservation laws (2.2)-(2.3) and (2.5) are to be solved subject to initial conditions (3.4)-(3.6) to get $g_1, g_2, m, \mathbf{u}$ and $\mathbf{v}$ for all time $t > 0$. The unit normal $\mathbf{n}$ can be determined from (2.1) once $\mathbf{u}$ and $\mathbf{v}$ are known. The ray equations (3.2) can then be integrated numerically with (3.3) as the initial condition to obtain the successive position and geometry of the wavefront Ω_t, see also [24].

4. Numerical Approximation

Due to the fact that we have an incomplete set of eigenvectors the system (2.2)-(2.3), (2.5) is weakly hyperbolic. Thus it is not well-posed in the strong hyperbolic sense and likely to be more sensitive than regular hyperbolic systems. This is also reflected in difficulties with obtaining a stable numerical approximation as we will see in Section 6, cf. second test case. The existence of the solution to weakly hyperbolic systems is an open problem in general. Numerical as well as theoretical analysis indicates that the solution does not belongs to BV spaces and is only measured valued. Clearly, due to the fact that we have a multiple eigenvalue $\lambda = 0$ typically δ function appears in the corresponding fields, which are linearly degenerate in our case. In addition they interact with the genuinely nonlinear field, that typically obtains shock. This yields the product of δ function with Heaviside distribution, which can be defined using measure theory. In literature one can find several publications, where such solutions have been studied for certain weakly hyperbolic systems, see [6, 8, 9, 10, 11, 13, 27, 28, 29] and the references therein, see also [7, 18] for numerical approximations of a certain systems. In our subsequent paper we want to study theoretically simplified model problems corresponding to the 3D-KCL system. For example, our goals will be construction of a solution to the Riemann problem or analytical results on existence of measure-valued solution. The aim of this section is to present a numerical solution of the KCL (2.2)-(2.3) and (2.5) using simple but robust central schemes. In particular we work with the first order staggered Lax-Friedrichs scheme and the second order Nessyahu-Tadmor scheme [23].

Note that the KCL (2.2)-(2.3) and the energy equation (2.5) for the variable $U = (u_1, u_2, v_1, v_2, m, g_1, g_2)^T$ can be written as a system of conservation laws

$$(H(U))_t + (F_1(U))_{\xi_1} + (F_2(U))_{\xi_2} = 0, \tag{4.1}$$

where

$$H(U) = \Big(g_1u_1, g_1u_2, g_1u_3, g_2v_1, g_2v_2, g_2v_3, (m-1)^2e^{2(m-1)}g_1g_2\sin\chi\Big)^T,$$
$$F_1(U) = (mn_1, mn_2, mn_3, 0, 0, 0, 0)^T,\ F_2(U) = (0, 0, 0, mn_1, mn_2, mn_3, 0)^T.$$

We briefly review the staggered Lax-Friedrichs scheme and the Nessyahu-Tadmor scheme for the system of conservation laws (4.1), see [1, 14, 15, 16, 23] for more details.

We denote the mesh points by $\xi_{1_i} = i\Delta\xi_1, \xi_{2_j} = j\Delta\xi_2, t_n = n\Delta t, i, j, \in \mathbb{Z}, n \in \mathbb{N}$. Let U_{ij}^n be an approximation to $U(i\Delta\xi_1, j\Delta\xi_2, n\Delta t)$. Note that the staggered schemes make use of two types of grids. At odd time steps we use the original mesh cells,

$$C_{i,j} = \Big[\xi_{1_{i-\frac{1}{2}}}, \xi_{1_{i+\frac{1}{2}}}\Big] \times \Big[\xi_{2_{j-\frac{1}{2}}}, \xi_{2_{j+\frac{1}{2}}}\Big]$$

and at even time steps the so-called dual or staggered grid is used

$$C_{i+\frac{1}{2},j+\frac{1}{2}} = \big[\xi_{1_i}, \xi_{1_{i+1}}\big] \times \big[\xi_{2_j}, \xi_{2_{j+1}}\big],$$

see Figure 1.

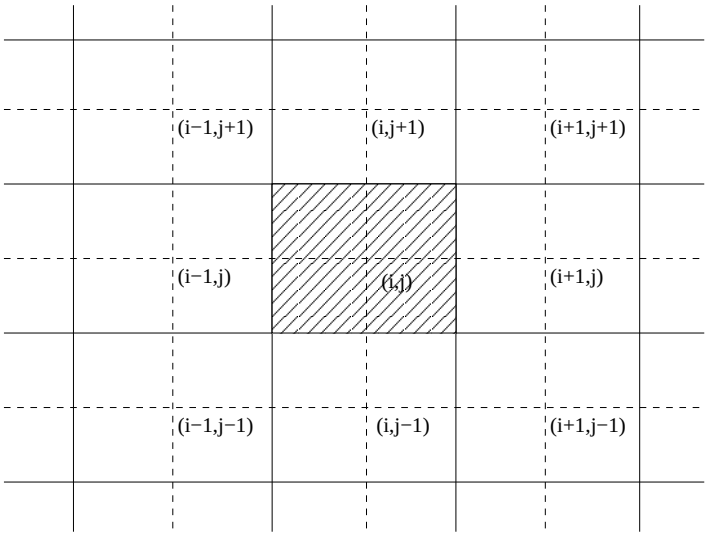

FIGURE 1. Computational stencil: the original grid is depicted by solid lines and a dual grid is denoted by dotted lines.

4.1. **Lax-Friedrichs Scheme.** In the staggered version the Lax-Friedrichs method produces the cell average at time t^{n+1} as given by

$$\begin{aligned} H(U^{n+1}_{i+\frac{1}{2},j+\frac{1}{2}}) =& \frac{1}{4}\left\{H(U^n_{i,j}) + H(U^n_{i+1,j}) + H(U^n_{i,j+1}) + H(U^n_{i+1,j+1})\right\} \\ &- \frac{\lambda_1}{2}\left\{F_1(U^n_{i+1,j}) - F_1(U^n_{i,j}) + F_1(U^n_{i+1,j+1}) - F_1(U^n_{i,j+1})\right\} \\ &- \frac{\lambda_2}{2}\left\{F_2(U^n_{i,j+1}) - F_2(U^n_{i,j}) + F_2(U^n_{i+1,j+1}) - F_2(U^n_{i+1,j})\right\}, \end{aligned} \tag{4.2}$$

where $\lambda_i = \Delta t/\Delta\xi_i, i = 1, 2$ are the mesh ratios. The cell average $H(U^{n+1}_{i,j})$ at the original mesh is obtained by interpolating the staggered cell averages

$$H(U^{n+1}_{i,j}) = \frac{1}{4}\left\{H(U^{n+1}_{i+\frac{1}{2},j+\frac{1}{2}}) + H(U^{n+1}_{i-\frac{1}{2},j+\frac{1}{2}}) + H(U^{n+1}_{i-\frac{1}{2},j-\frac{1}{2}}) + H(U^{n+1}_{i+\frac{1}{2},j-\frac{1}{2}})\right\}. \tag{4.3}$$

4.2. **Nessyahu-Tadmor Scheme.** The Nessyahu-Tadmor scheme [1, 14, 15, 23] is a second order TVD extension of the Lax-Friedrichs scheme. It is a two step predictor-corrector method. In the predictor step we compute the value of the conserved variable at half time step

$$H(U^{n+\frac{1}{2}}_{i,j}) = H(U^n_{i,j}) - \frac{\lambda_1}{2}F_1(U^n_{i,j})' - \frac{\lambda_2}{2}F_2(U^n_{i,j})`, \tag{4.4}$$

where $(\cdot)' \approx \Delta\xi_1\partial_{\xi_1}(\cdot)$ and $(\cdot)` \approx \Delta\xi_2\partial_{\xi_2}(\cdot)$ are suitable finite difference operators. For example, the slopes can be approximated using the minmod limiter in the following way

$$(F_1{}^n_{i,j})' = MM\left\{\theta\left(F_1{}^n_{i+1,j} - F_1{}^n_{i,j}\right), \frac{1}{2}\left(F_1{}^n_{i+1,j} - F_1{}^n_{i-1,j}\right), \theta\left(F_1{}^n_{i,j} - F_1{}^n_{i-1,j}\right)\right\},$$

$$(F_2{}^n_{i,j})` = MM\left\{\theta\left(F_2{}^n_{i,j+1} - F_2{}^n_{i,j}\right), \frac{1}{2}\left(F_2{}^n_{i,j+1} - F_2{}^n_{i,j-1}\right), \theta\left(F_2{}^n_{i,j} - F_2{}^n_{i,j-1}\right)\right\}.$$

We have denoted $F_{k\,i,j}^{n} = F_k(U_{i,j}^n)$, for $k = 1, 2$, the parameter θ takes values in $[1, 2]$. The minmod function is defined by

$$MM\{v_1, v_2, \cdots\} = \begin{cases} \min_p\{v_p\} & \text{if } v_p > 0 \ \forall p, \\ \max_p\{v_p\} & \text{if } v_p < 0 \ \forall p, \\ 0 & \text{otherwise.} \end{cases}$$

In the corrector step of the Nessyahu-Tadmor scheme the staggered average $H(U^{n+1}_{i+\frac{1}{2},j+\frac{1}{2}})$ at time t^{n+1} is updated as follows

$$\begin{aligned} H(U^{n+1}_{i+\frac{1}{2},j+\frac{1}{2}}) =& H(U^{n}_{i+\frac{1}{2},j+\frac{1}{2}}) \\ &- \frac{\lambda_1}{2}\left\{F_1(U^{n+\frac{1}{2}}_{i+1,j}) - F_1(U^{n+\frac{1}{2}}_{i,j}) + F_1(U^{n+\frac{1}{2}}_{i+1,j+1}) - F_1(U^{n+\frac{1}{2}}_{i,j+1})\right\} \\ &- \frac{\lambda_2}{2}\left\{F_2(U^{n+\frac{1}{2}}_{i,j+1}) - F_2(U^{n+\frac{1}{2}}_{i,j}) + F_2(U^{n+\frac{1}{2}}_{i+1,j+1}) - F_2(U^{n+\frac{1}{2}}_{i+1,j})\right\}. \end{aligned} \tag{4.5}$$

Note that we use a piecewise linear reconstruction of the conserved variable $H(U^n_{i,j})$ on the original grid

$$H\left(U(\xi_1, \xi_2, t^n)\right) = H(U^n_{i,j}) + \frac{(\xi_1 - \xi_{1i})}{\Delta\xi_1} H(U^n_{i,j})' + \frac{(\xi_2 - \xi_{2j})}{\Delta\xi_2} H(U^n_{i,j})\backprime, \tag{4.6}$$

where the slopes are computed as

$$\begin{aligned} (H^n_{i,j})' &= MM\left\{\theta\left(H^n_{i+1,j} - H^n_{i,j}\right), \frac{1}{2}\left(H^n_{i+1,j} - H^n_{i-1,j}\right), \theta\left(H^n_{i,j} - H^n_{i-1,j}\right)\right\}, \\ (H^n_{i,j})\backprime &= MM\left\{\theta\left(H^n_{i,j+1} - H^n_{i,j}\right), \frac{1}{2}\left(H^n_{i,j+1} - H^n_{i,j-1}\right), \theta\left(H^n_{i,j} - H^n_{i,j-1}\right)\right\}. \end{aligned}$$

Here $H^n_{i,j}$ is a shortcut for $H(U^n_{i,j})$. Now the staggered average $H(U^n_{i+\frac{1}{2},i+\frac{1}{2}})$ at the time level t^n can be obtained by averaging the linear functions (4.6)

$$\begin{aligned} H(U^n_{i+\frac{1}{2},j+\frac{1}{2}}) =& \frac{1}{4}\left\{H(U^n_{i,j}) + H(U^n_{i+1,j}) + H(U^n_{i+1,j+1}) + H(U^n_{i,j+1})\right\} \\ &+ \frac{1}{16}\left\{H(U^n_{i,j})' - H(U^n_{i+1,j})' - H(U^n_{i+1,j+1})' + H(U^n_{i,j+1})'\right\} \\ &+ \frac{1}{16}\left\{H(U^n_{i,j})\backprime + H(U^n_{i+1,j})\backprime - H(U^n_{i+1,j+1})\backprime - H(U^n_{i,j+1})\backprime\right\}. \end{aligned} \tag{4.7}$$

Finally the cell average $H(U^{n+1}_{i,j})$ is obtained by linear interpolation of the staggered averages $H(U^n_{i+\frac{1}{2},j+\frac{1}{2}})$ and by averaging, [15]

$$\begin{aligned} H^{n+1}_{i,j} =& \frac{1}{4}\left\{H^{n+1}_{i+\frac{1}{2},j+\frac{1}{2}} + H^{n+1}_{i-\frac{1}{2},j+\frac{1}{2}} + H^{n+1}_{i-\frac{1}{2},j-\frac{1}{2}} + H^{n+1}_{i+\frac{1}{2},j-\frac{1}{2}}\right\} \\ &+ \frac{1}{16}\left\{\left(H^{n+1}_{i-\frac{1}{2},j-\frac{1}{2}}\right)' - \left(H^{n+1}_{i+\frac{1}{2},j-\frac{1}{2}}\right)' + \left(H^{n+1}_{i-\frac{1}{2},j+\frac{1}{2}}\right)' - \left(H^{n+1}_{i+\frac{1}{2},j+\frac{1}{2}}\right)'\right\} \\ &+ \frac{1}{16}\left\{\left(H^{n+1}_{i-\frac{1}{2},j-\frac{1}{2}}\right)\backprime - \left(H^{n+1}_{i-\frac{1}{2},j+\frac{1}{2}}\right)\backprime + \left(H^{n+1}_{i+\frac{1}{2},j-\frac{1}{2}}\right)\backprime - \left(H^{n+1}_{i+\frac{1}{2},j+\frac{1}{2}}\right)\backprime\right\}. \end{aligned} \tag{4.8}$$

Notice that both the Lax-Friedrichs scheme (4.2) and the Nessyahu-Tadmor scheme (4.5) give the update for $H(U^{n+1}_{i,j})$. In order to get the values of the variables $m, g_1, g_2, \mathbf{u}$ and $\mathbf{v}$ we need to employ an appropriate nonlinear solver. In our numerical experiments a fix point iteration has been used in (2.5). After computing the normal vector $\mathbf{n}$ from (2.1) we integrate the ray equations (3.2) to determine the wavefront at new time t^{n+1}. Here we have used the compound trapezoidal rule for the numerical integration in time.

6. Numerical experiments

In order to demonstrate applicability of the 3-D KCL for modelling of time evolution of nonlinear wavefronts we present in this section two illustrating examples. An interesting phenomena such as a kink line and a point singularity can be noticed in the physical $(x_1, x_2, x_3)-$space. On the other hand the resulting functions in the ray coordinates still remain single valued.

In the **first test case** the initial wavefront Ω_0 has the shape of a Gaussian pulse

$$\Omega_0 \colon x_3 = e^{-(x_1^2+x_2^2)} \equiv f(x_1, x_2). \tag{6.1}$$

On Ω_0 the ray coordinates ξ_1 and ξ_2 can be chosen to be

$$\xi_1 = x_1, \quad \xi_2 = x_2. \tag{6.2}$$

Using (3.5)-(3.6) the initial values for the metrics g_1, g_2 and the vectors $\mathbf{u}$ and $\mathbf{v}$ can be obtained to be

$$g_{1_0} = \left(1 + f_{\xi_1}^2\right)^{1/2}, \quad g_{2_0} = \left(1 + f_{\xi_2}^2\right)^{1/2}. \tag{6.3}$$

$$\mathbf{u}_0 = \frac{1}{g_1}\left(1, 0, f_{\xi_1}\right), \quad \mathbf{v}_0 = \frac{1}{g_2}\left(0, 1, f_{\xi_2}\right). \tag{6.4}$$

The initial value of m is set to $m_0 = 1.2$. The computational domain is taken to be the square $[-5, 5]\times[-5, 5]$ and time evolution of nonlinear wavefront is calculated up to the final time $t = 2.5$. We have used a grid with 200×200 cells. In order to keep the method stable the following CFL stability condition has been used

$$\frac{\Delta t}{h} \max(\rho_1, \rho_2) \leq \text{CFL},$$

where $h = \Delta\xi_1 = \Delta\xi_2$ is a mesh step and ρ_1, ρ_2 are respectively maximum generalized eigenvalues of the Jacobian matrices $B^{(1)}$ and $B^{(2)}$ with respect to A, cf. (2.6). Here we have taken the CFL number 0.45. For the generalized limiter defined in the Subsection 4.2 the parameter θ was set to 2.

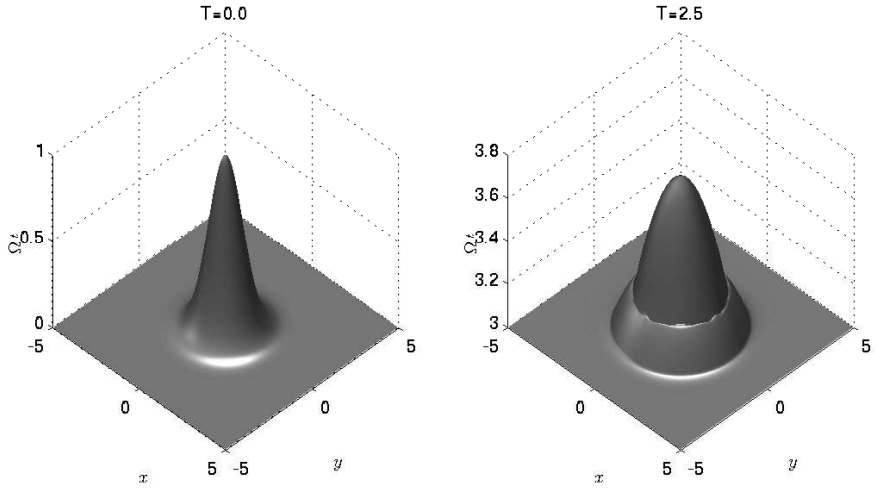

Figure 2. The nonlinear wavefront Ω_t starting initially in the shape of a Gaussian elevation.

In Figure 2 we show the surface plot of the initial wavefront Ω_0 and the wavefront Ω_t at time $t = 2.5$. The wavefront at $t = 2.5$ has moved up in the x_3-direction and has spread over a larger area in (x_1, x_2)-plane and its height has decreased. The two kink circles are clearly seen as sharp lines, one at the base $x_3 = 3$ and

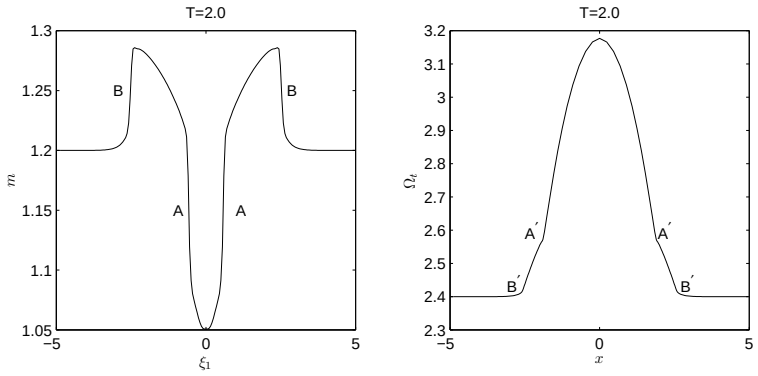

FIGURE 3. The kink lines A' and B' in (x_1, x_2, x_3)-space are images of shocks A and B in the ray coordinate system.

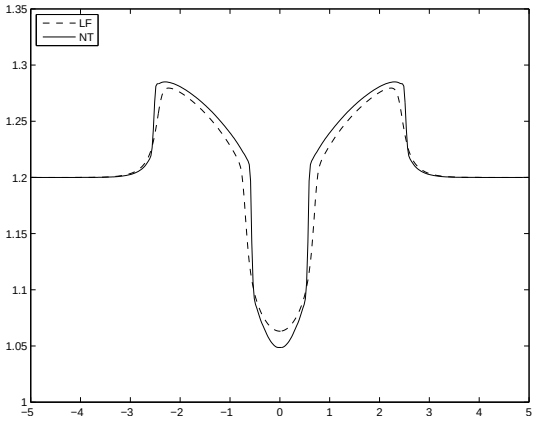

FIGURE 4. Time evolution of m at the cross-section $\xi_2 = 0$ for $t = 2.5$ obtained by the Lax-Friedrichs and the Nessyahu-Tadmor methods.

another above it. As already mentioned in the Section 4 the position of Ω_t has been obtained by numerical integration of the ray equations (3.2).

In Figure 3 we plot the graph of $m = m(\xi_1)$ in $\xi_2 = 0$ plane and the shape of Ω_t with respect to x_1 in the cross-section $x_2 = 0$ at time $t = 2.0$. From the $(m - \xi)$ graph we find two shocks A and B (which would become shock circles in (m, ξ_1, ξ_2)-space). These shocks map onto two kinks A' and B' (or kink circles in (x_1, x_2, x_3)-space). For a detailed discussion on the formation and propagation of kinks in a two dimensional problem and resolution of a caustic due to nonlinearity a reader is referred to [4, 21, 24, 26].

Next we present the time evolution of the normal velocity m and metrics g_1, g_2 with respect to ξ_1 (in $\xi_2 = 0$ plane) in Figures 4, 5, 6 and 7. In Figure 4 both results obtained by the the Lax-Friedrichs scheme and by the Nessyahu-Tadmor are plotted. As expected the second order Nessyahu-Tadmor resolves shocks more sharply. In the following pictures we just present the results obtained by the second order Nessyahu-Tadmor scheme.

From the plots of m, g_1 and g_2 we find that when m decreases (increases) the value of g_1 increases (decreases) but the value of g_2 always keeps on increasing in $\xi_2 = 0$ plane. However, all these changes remain consistent with the conservation law (2.5), which states that $(m-1)^2 e^{2(m-1)} g_1 g_2 \sin\chi = \text{const}$. We have not given

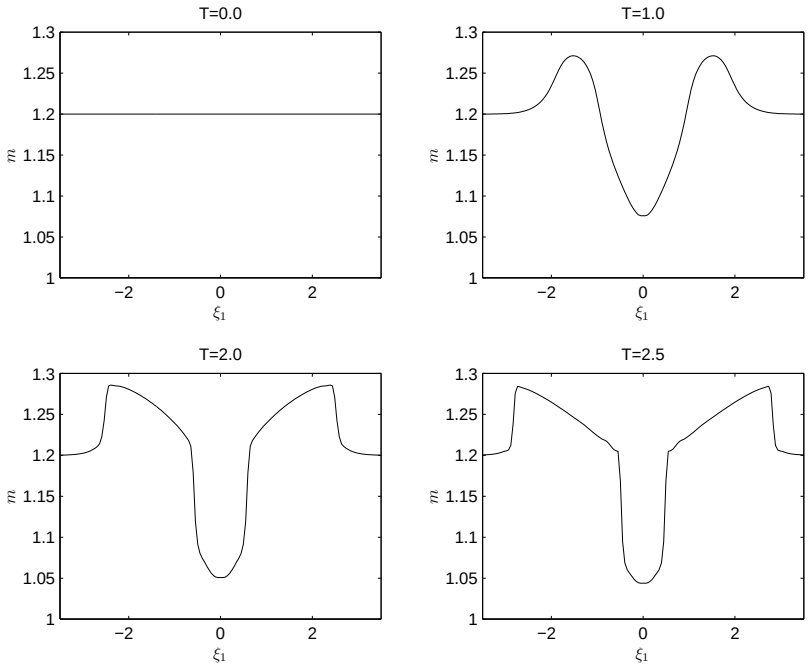

FIGURE 5. Time evolution of m at the cross-section $\xi_2 = 0$.

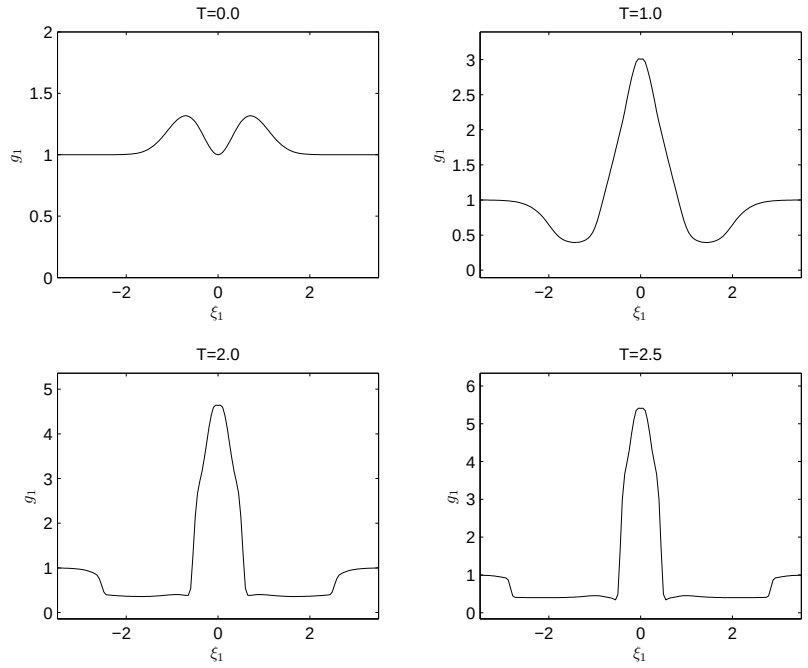

FIGURE 6. Time evolution of the metric g_1 at the cross-section $\xi_2 = 0$.

the graph of χ. From the results of m and g_1 it is clear that the shocks arise between $t = 1$ and $t = 2$.

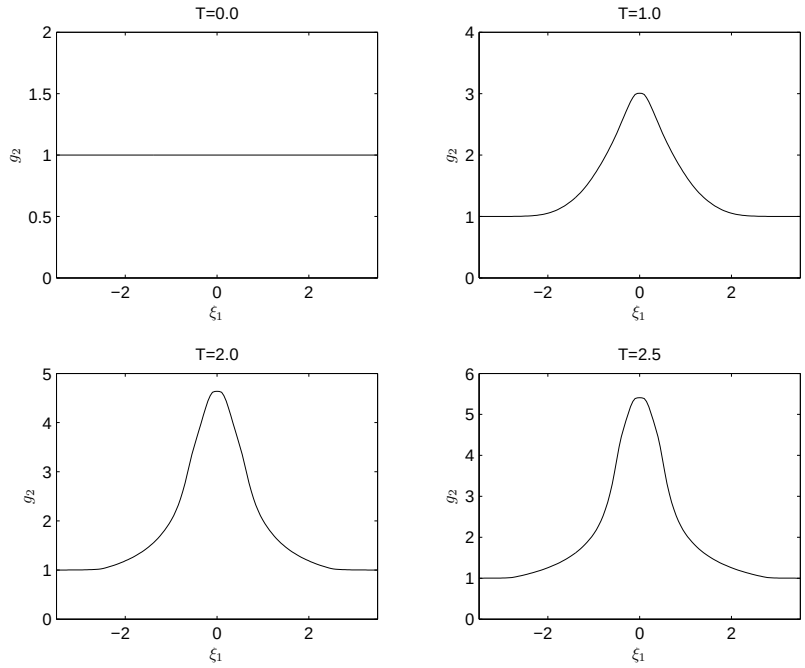

FIGURE 7. Time evolution of the metric g_2 at the cross-section $\xi_2 = 0$.

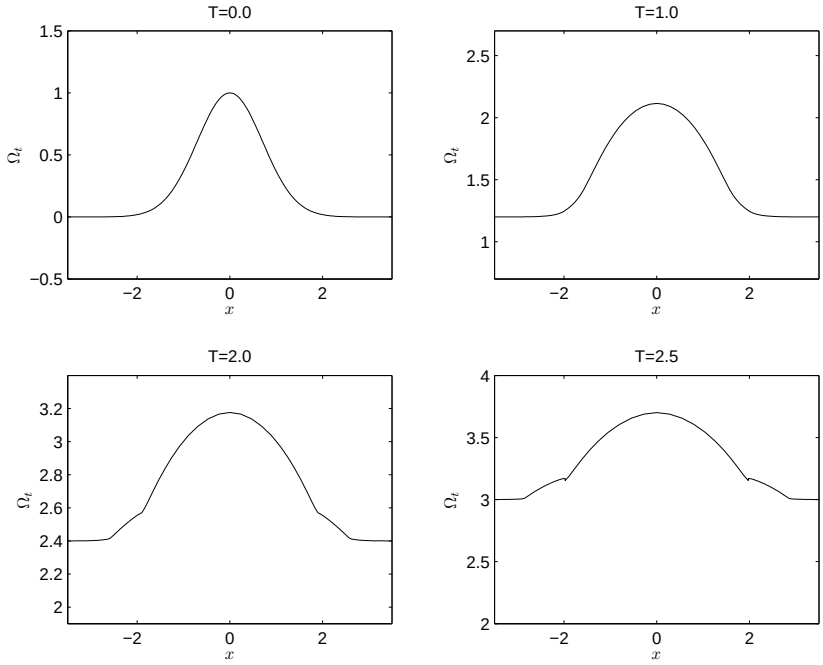

FIGURE 8. Time evolution of the geometry and position of the nonlinear wavefront Ω_t at cross-section $x_2 = 0$.

Now we present the results in physical space (x_1, x_2, x_3)-space. The surface plot has already been given in Figure 2. However, to get the more detailed view on

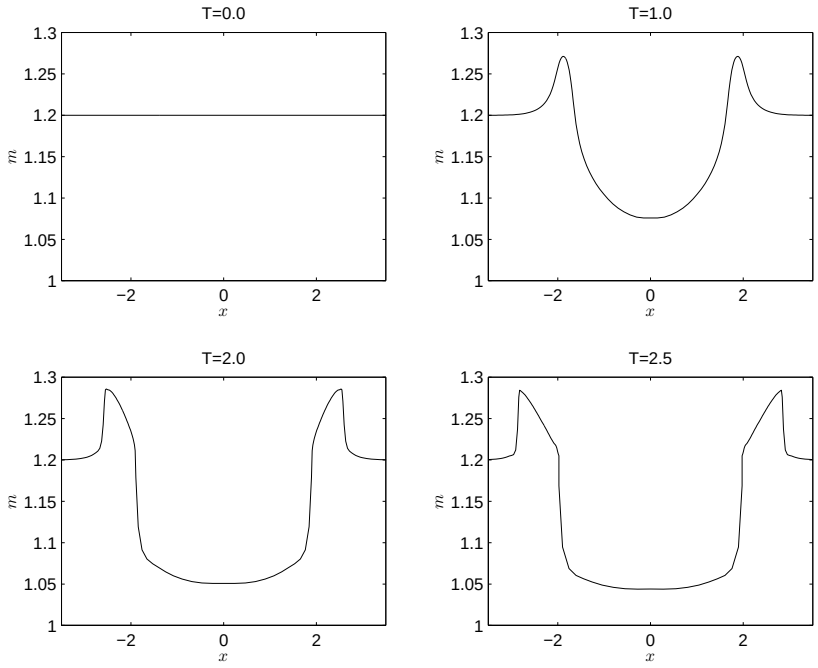

FIGURE 9. Time evolution of the normal velocity m at the cross-section $x_2 = 0$.

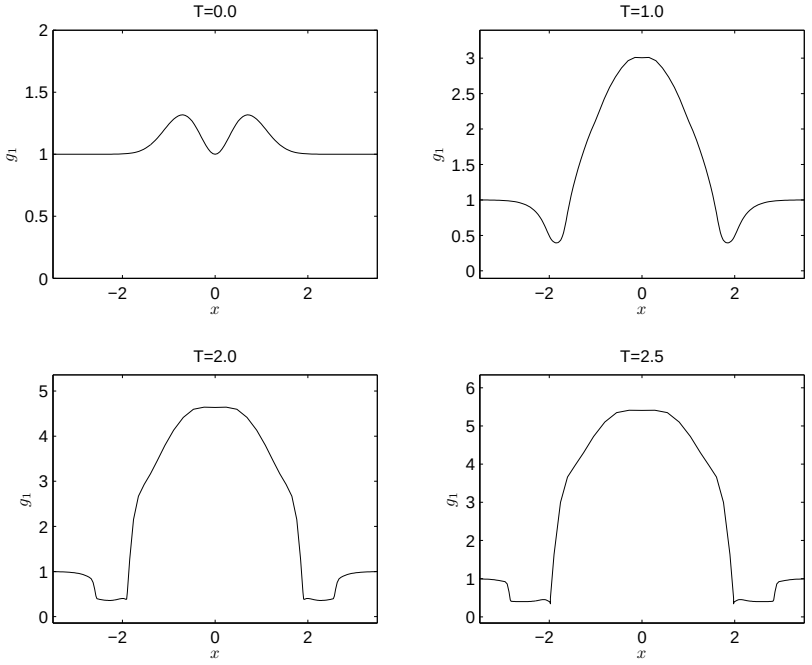

FIGURE 10. Time evolution of the metric g_1 at the cross-section $x_2 = 0$.

structures of Ω_t we plot sections of Ω_t, m, g_1 and g_2 with respect to x_1 at $x_2 = 0$ plane. The two kinks are clearly visible at $t = 2.0$ and $t = 2.5$. The upper part of

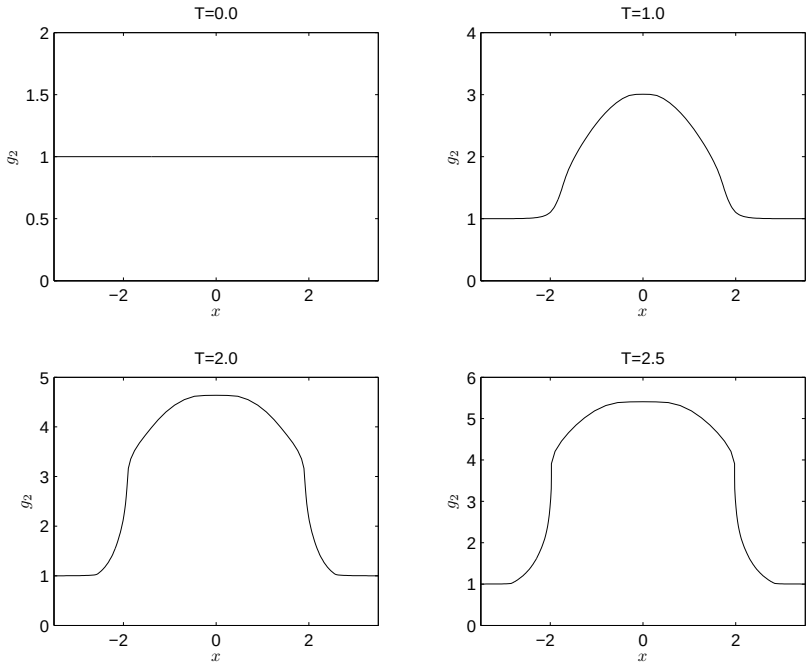

FIGURE 11. Time evolution of the metric g_2 at the cross-section $x_2 = 0$.

Ω_0 is clearly convex upward and rays diverge leading to a decrease in the value of m. However, near the base $x_3 = 0$, one principal curvature is positive but other negative. The kink lines are formed as circles. At $t = 2.5$ there appears to be a complex geometry near the upper kink circle as seen in Figures 8 and 10. It is interesting that the 3-D KCL are able to give such finer details.

Furthermore, it is worth remarking that the KCL reduce the original problem of evolution of Ω_t in four dimensions (x_1, x_2, x_3, t) to that in three dimensions in (ξ_1, ξ_2, t)-space. This reduces the computational cost considerably and hence many practical problems can be solved more efficiently.

In the **second test case** an initial wavefront Ω_0 is taken to be axi-symmetric paraboloid extended by a tangent conoid given in the following way

$$x_3 = \begin{cases} \left(x_1^2 + x_2^2\right), & \text{if} \quad (x_1^2 + x_2^2)^{1/2} \leq 1, \\ 2(x_1^2 + x_2^2)^{1/2} - 1, & \text{otherwise.} \end{cases}$$

In [21] an analogous 2D-test problem has been considered. However, in 3D-case we have observed stronger singularity leading to numerical instabilities for large t. In Figure 12 the computational results obtained by the Lax-Friedrichs scheme up to $t = 1.5$ are presented. We have used a grid with 100×100 cells and had to set the CFL number to 0.15. We have numerically solved this problem also by NT scheme. the results look physically realistic and agrees with the results by LF scheme up to time $t = 0.4$. Then some unphysical features start appearing between $t = 0.4$ and $t = 0.5$, we claim it to be unphysical after comparing with the LF scheme. We do not give these results here as we like to investigate thoroughly the reasons of the failure of NT scheme.

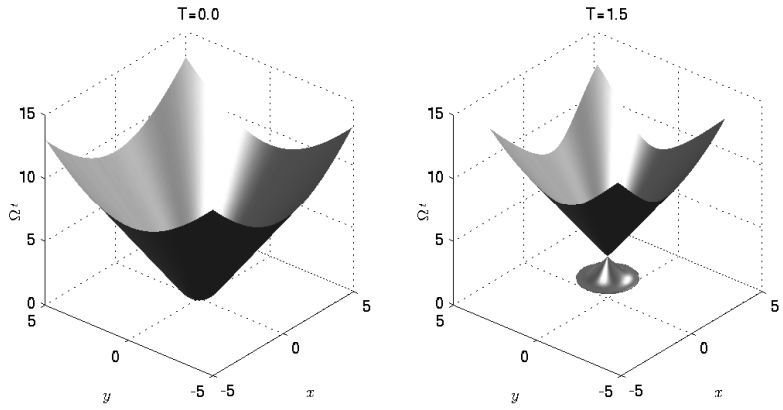

FIGURE 12. Time evolution of the nonlinear wavefront having initially the form of a paraboloid; graphs of solution at $t = 0.0$ and $t = 1.5$.

This example presents a new challenge which we shall study and report in subsequent papers. Our future goal is to investigate the propagation of a curved nonlinear wavefront where the converging effects and appearance of analogous singularities are dominant. This may lead to the formation of δ waves similar to δ shocks. Our emphasis would be to study this situation more closely from theoretical as well as computational point of view and design robust and stable numerical algorithms. The main aim of the present paper was to present illustrating experiments showing that the 3-D KCL is a useful tool to study evolution of moving surfaces.

7. Acknowledgement

The authors sincerely thank Phoolan Prasad, IISc Bangalore, for his encouragement and valuable discussions. We also thank the Department of Science and Technology (DST), Goverment of India and the German Academic Exchange Service (DAAD) for the financial support of our collaborative research. K. R. Arun would like to express his gratitude to the Council of Scientific & Industrial Research (CSIR) for supporting his research at the Indian Institute of Science under the grant-09/079(2084)/2006-EMR-1. Department of Mathematics of IISc is supported by UGC under SAP.

References

[1] Arminjon P, Viallon M C and Madrane A. A finite volume extension of the Lax-Friedrichs and Nessyahu-Tadmor schemes for conservation laws on unstructured grids. *Int. J. Comp. Fluid Dyn.* 9:1-22, 1997.

[2] Arun K R and Prasad P. 3-D Kinematical Conservation Laws (KCL): Equations of evolution of a surface. *Preprint*No. 33, 2007, Department of Mathematics, Indian Institute of Science, Bangalore, available on `http://math.iisc.ernet.in/%7Eeprints/`

[3] Baskar S and Prasad P. Kinematical conservation laws applied to study geometrical shapes of a solitary wave. *Wind over waves II: Forcasting and Fundamentals*. Sajjadi S and Hunt J (eds.), Horwood Publishing Ltd, pp.189-200, 2003.

[4] Baskar S and Prasad P. Propagation of curved shock fronts using shock ray theory and comparison with other theories. *J. Fluid Mech.* 523:171-198, 2005.

[5] Baskar S and Prasad P. Formulation of the problem of sonic boom by a maneuvering aerofoil as a one parameter family of Cauchy problems. *Proceedings of Indian Academy of Sciences: Mathematical sciences*. 116:97-119, 2006.

[6] Bouchut F. On zero pressure gas dynamics. In *Advances in Kinetic Theory and Computing*, volume 22 of *Ser. Adv. Math. Appl. Sci.*, pp.171-190. World Sci. Publishing, River Edge, NJ, 1994.

[7] Bouchut F, Jin S and Li X. Numerical approximations of pressureles and isothermal gas dynamics, *SIAM J. Num. Anal.*, 41:135-158, 2003.
[8] Brenier Y and Grenier E. Sticky particles and scalar conservation laws. *SIAM J. Num. Anal.* 35:2317-2328, 1998.
[9] Chen G Q and Kan P T. Hyperbolic conservation laws with umbilic degeneracy (I). *Arch. Rat. Mech. Anal.* 130:231-276, 1995.
[10] Danilov V. G and Mitrovic D.Delta shock wave formation in the case of triangular hyperbolic system of conservation laws. *to appear in J. Diff. Equations*, avialable on `http//www.math.ntnu.no/conservation/2006/057.html`
[11] Enquist B and Runborg O. Multi-phase computations in geometrical optics. *J. Comp. Appl. Math.* 74:175-192, 1996.
[12] Giles M, Prasad P and Ravindran R. Conservation form of equations of three dimensional front propagation. *Technical Report, Department of Mathematics, Indian Institute of Science* 1995.
[13] Huang, F. Existence and uniqueness of discontinuous solutions for a class of nonstrictly hyperbolic systems, *Advances in Nonlinear Partial Differential Equations and Related Areas*, Beijing 1997, 187-208, World Sci. Publ., River Edje, NJ, 1998.
[14] Jiang G S and Tadmor E. Nonoscillatory central schemes for multidimensional hyperbolic conservation laws. *SIAM J. Sci. Comp.* 19:1892-1917, 1995.
[15] Jiang G. S, Levy D, Lin C T, Osher S and Tadmor E. High-resolution nonoscillatory central schemes with nonstaggered grids for hyperbolic conservation laws. *SIAM J. Num. Anal.* 35:2147-2168, 1998.
[16] Lax P. Weak solutions of nonlinear hyperbolic equations and their numerical computation. *Comm. Pure Appl. Math.* 7:159-193, 1954.
[17] LeFloch P. G. An existence and uniqueness result for two nonstrictly hyperbolic systems. *IMA Volumes in Math. and its Appl., "Nonlinear evolution equations that change type"*. Keyfitz B. L and Shearer M (eds.), Springer Verlag, Vol. 27, pp.126–138, 1990.
[18] LeVeque R. J. The dynamics of pressureless dust clouds and delta waves. *J. Hyper. Diff. Equat.* 1: 315-327, 2004.
[19] Liu T. P and Zin Z. Stability of viscous shock waves associated with a system of nonstrictly hyperbolic conservations laws. *Commu. Pure Appl. Math.* 45:361-388, 2006.
[20] Majda A and Zheng Y. Existence of global weak solutions to one-component vlasov-poisson and fokker-planck-poisson systems in one space dimension with measures as initial data. *Commu. Pure Appl. Math.* 47:1365-1401, 2006.
[21] Monica A and Prasad P. Propagation of a curved weak shock. *J. Fluid Mech.* 434:119-151, 2001.
[22] Morton K W, Prasad P and Ravindran R. Conservation form of nonlinear ray equations. *Technical report No.2, Department of Mathematics, Indian Institute of Science Bangalore.* 1992.
[23] Nessyahu H and Tadmor E. Non-oscillatory central differencing for hyperbolic conservation laws. *J. Comp. Phys.* 87:408-463, 1990.
[24] Prasad P. Nonlinear hyperbolic waves in multi-dimensions. *Monographs and Surveys in Pure and Applied Mathematics, Chapman and Hall/CRC, 121*, 2001.
[25] Prasad P. Kinematical conservation laws, ray theories and applications. *Indian J. Pure and Appl. Math.* 38:467-490, 2007.
[26] Prasad P and Sangeeta K. Numerical simulation of converging nonlinear wavefronts. *J. Fluid Mech.* 385:1-20, 1999.
[27] Shelkovich V. M. Multidimensional delta-shocks and the transportation and concentration processes. Preprint 2007, available on `http://www.math.ntnu.no/conservation/2007/031.html`
[28] Runborg O. Some new results in multiphase geometrical optics. *M2AN Math. Model. Numer. Anal.* 34:1203-1231, 2000.
[29] Tan D, Zhang T and Zheng Y. X. Delta-shock waves as limits of vanishing viscosity for hyperbolic systems of conservation laws. *J. Diff. Equations.* 112:1-32, 1994.

(K. R. Arun) Department of Mathematics, Indian Institute of Science, Bangalore, India-560012.

(M. Lukáčová-Medviďová) Institute of Numerical Simulation, Hamburg University of Technology, D-21071 Hamburg, Germany.
E-mail address: lukacova@tu-harburg.de
URL: www.tu-harburg.de/ins/hp/lukacova/

(S. V. Raghurama Rao) Department of Aerospace Engineering, Indian Institute of Science, Bangalore, India-560012.
E-mail address: raghu@aero.iisc.ernet.in